

## EXTENDING THE CORRELATION OF $L_R - L_X$ TO GAMMA RAY BURSTS

JING LÜ<sup>1,2</sup>, JING-WEN XING<sup>3</sup>, YUAN-CHUAN ZOU<sup>3</sup>, WEI-HUA LEI<sup>3</sup>, QINGWEN WU<sup>3</sup>, AND DING-XIONG WANG<sup>3</sup>

*Draft version March 4, 2022*

### ABSTRACT

The well-known correlation between the radio luminosity ( $L_R$ ) and the X-ray luminosity ( $L_X$ )  $L_R/L_X \simeq 10^{-5}$  holds for a variety of objects like active galactic nuclei, galactic black holes, solar flares and cool stars. Here we extend the relation to gamma-ray bursts (GRBs), and find the GRBs also lay on the same  $L_R - L_X$  relation, with a slightly different slope as  $L_R \propto L_X^{1.1}$ . This relation implies the explosions in different scales may have common underlying origin.

*Subject headings:* gamma-ray: bursts, AGN, black hole

### 1. INTRODUCTION

With the enhancement of the observational instruments, more and more astronomical objects have been discovered continuum radiation from the radio to the X-rays, including active galactic nuclei (AGN) (Sanders et al. 1989; Merloni et al. 2003), the Sun, cool star (Güdel & Benz 1993) and gamma ray burst (GRB) (Kumar & Zhang 2015), for instance. Recently, the relation between the radio and X-ray emission among different scale objects obtained much attention. The radio flares and soft X-rays of dwarf M-star UV Ceti were observed simultaneously by VLA and ROSAT/HRI telescope respectively (Benz et al. 1996). For active cool stars, Güdel & Benz (1993) gave a tight correlation between the quiescent radio and X-ray emission, where  $L_R/L_X \sim 10^{-5}$ , known as the Güdel-Benz relation. During the ROSAT All-Sky Survey accompanied by mostly simultaneous VLA observations, Güdel et al. (1993b) also gave a tight correlation between radio and X-ray luminosities of M dwarfs. Benz & Güdel (1994) showed the soft X-ray and radio luminosities of solar flares and the coronae of main-sequence, late-type stars follow the relation,  $L_{\nu,X}/L_{\nu,R} = k \times 10^{15.5 \pm 0.5}$ , where  $k$  is a coefficient and different types of stars have different values. Linsky (1996) suggested that the heating mechanism of stellar corona is a flare-like process, and in the review, van den Oord (1999) discussed various aspects of stellar flares. Güdel & Benz (1996) discussed a few aspects of radio and X-ray studies of solar-like stars, and gave that nonthermal radio and thermal soft X-ray emissions from solar-like stars provided direct information on particle acceleration and coronae heating in the magnetically confined outer atmospheres. Laor & Behar (2008) found that there is a more tight correlation between the radio and X-ray fluxes of accretion disks in radio-quiet quasars as in coronally active stars,  $L_R/L_X \lesssim 10^{-5}$  (with a  $1\sigma$  scatter of about a factor of 3 in  $L_R$ ). They proposed that most of the radio emission might come from coronae, and

the coronae are magnetically heated. Middleton et al. (2013) showed that the X-ray and radio emission are coupled in some sources. Continued radio and X-ray monitoring of some sources should reveal the causal relationship between the accretion flow and the powerful jet emission. Here we try to extend the  $L_R - L_X$  relation to GRBs.

GRBs are high energy  $\gamma$ -rays lasting from several milliseconds to a few thousand seconds, and they are the most powerful explosions in the universe (Piran 2004; Zhang 2007). GRBs were discovered in the late 1960s by the military Vela satellites (Klebesadel et al. 1973), and caused the great interests of people afterwards. Because the duration of the GRB explosion is very short, the precise location can not be determined in the beginning. Also BeppoSAX satellite, launched on 30 April 1996, confirmed the cosmological distance of GRBs in 1997 (Kumar & Zhang 2015). With the launching of space missions (such as *Swift* and *Fermi*), they have greatly enriched our knowledge of this phenomenon. With the more and more observational data, statistical studies have summarized some empirical relationship, such as  $E_{peak} \sim E_{\gamma,iso}$  (Amati et al. 2002),  $E_{peak} \sim L_{\gamma,iso}$  (Yonetoku et al. 2004),  $E_{peak} \sim E_{\gamma}$  (Ghirlanda et al. 2004),  $E_{peak} \sim E_{\gamma,iso} \sim t_b$  (Liang & Zhang 2005),  $\Gamma_0 \sim E_{\gamma,iso}$  (Liang et al. 2010) and  $\Gamma_0 \sim L_{\gamma,iso}$  (Ghirlanda et al. 2012; Lü et al. 2012). A dedicated theoretical study for the  $\Gamma_0 - L_{\gamma,iso}$  relation suggests that it can be a justification of the central engine models of GRBs (Lei, Zhang & Liang 2013). Recently, Wu et al. (2011) found a uniform correlation between the synchrotron luminosity and Doppler factor for both GRBs and blazars, which implies that they may share some similar jet physics. The recent work by Wang et al. (2014) on Sw J1644+57 (a tidal disruption event candidate which launches a relativistic jet) may support this similarity. In their work, the radio light curve of Sw J1644+57 were the successfully interpreted with the afterglow jet model. The discovery of the long-lived afterglows at X-ray, optical and radio wavelengths advanced the study of large samples of GRBs. Chandra & Frail (2012) gave a catalog of radio afterglow of GRBs over a 14 year period from 1997 to 2011, and also include the 11hr X-ray observations in it. These progresses make it possible to extend the  $L_R - L_X$  relation to GRBs.

This paper is organized as follows. In section 2, we

<sup>1</sup> GXU-NAOC Center for Astrophysics and Space Sciences, Department of Physics, Guangxi University, Nanning 530004, China

<sup>2</sup> Guangxi Key Laboratory for Relativistic Astrophysics, Nanning 530004, China

<sup>3</sup> School of Physics, Huazhong University of Science and Technology, Wuhan, 430074, China. Email: zouyc@hust.edu.cn (YCZ)

give the samples selection and analysis of solar flares, cool stars, AGNs and GRBs data. We end with brief conclusion and discussion in section 3.

## 2. DATA AND ANALYSIS

We investigate the  $L_R \sim L_X$  relation of objects in different scales, including stars, AGNs, and GRBs. The data of the solar flares and cool stars are taken from Laor & Behar (2008), who tabulated the data of Benz & Güdel (1994). Solar flare soft X-rays are conventionally measured in a narrow and harder band than the stellar sources, and the data points from the solar flares are for different classes that may deviate from the overall linear relation Benz & Güdel (1994). We take the  $L_R$  and  $L_X$  of AGNs from Merloni et al. (2003).

Our analysis focus on  $L_R$  and  $L_X$  for GRBs. Based on the radio peak flux densities and luminosity distances  $D_L$  calculated from the redshift  $z$ , we can obtain the radio luminosity of GRBs afterglow,  $L_R \simeq 4\pi D_L^2 F_{\nu, m} \times \nu_R$ . For GRBs, we chose 47 samples with both radio and X-ray observations. They are listed in Table 1. Before GRB 111215A, 42 GRBs are taken from Chandra & Frail (2012). Also we can obtain bursts radio frequency and peak flux densities in their Table 3, X-ray flux at 11hr after burst in their Table 6. For the other five bursts we have used: GRB 111215A: van der Horst et al. (2015) for redshift, Zauderer et al. (2013) for radio peak flux density, and in it's Figure 3, there are five radio light curves at 5.8, 8.4, 19.1, 24.4 and 93GHz, but from their profiles, the first three may result from the positive and negative shock, and the remaining two may result from external shock, so we chose the peak flux density of 8.4GHz. GRB 120326A: Kruehler et al. (2012) for redshift, Staley et al. (2013) for radio peak flux density. GRB 130427A: Xu et al. (2013) and Flores et al. (2013) for redshift, Anderson et al. (2014) for radio peak flux density. GRB 130603B: Cucchiara et al. (2013) for redshift, Fong et al. (2014) for radio peak flux density. GRB 130907A: de Ugarte Postigo et al. (2013) for redshift, Veres et al. (2014) for radio peak flux density. The X-ray flux at 11hr of these five bursts are taken from Swift-XRT products for GRBs <sup>4</sup>.

In figure 1, we give the distribution of the 15 solar flares (black dot circles), 65 cool stars (blue stars), 149 AGNs (red triangles) and 47 GRBs (black solid circles) objects in the  $L_R \sim L_X$  plane. The black solid line in lower panel,  $L_R \simeq 3.42 \times 10^{-10} L_X^{1.122}$  is the best fit, and compared to the red dashed line,  $L_R = 10^{-5} L_X$ . Remarkably, all of them appear to follow a similar  $L_R \sim L_X$  relation, despite they span  $\sim 30$  orders of magnitude in luminosity between these different types of active objects.

We investigate the  $L_R \sim L_X$  relation mentioned by Benz & Güdel (1994) with our larger samples. Laor & Behar (2008) gave the linear relation  $\log L_{R,39} = (-0.21 \pm 0.08) + (1.08 \pm 0.15) \log L_{X,44}$  for radio quiet quasar (RQQ). In Figure 1, we plot the  $L_R$  and  $L_X$  on log log coordinates of our 276 samples, and gets a slightly modified relation

$$\log L_R = (-9.466 \pm 0.102) + (1.122 \pm 0.002) \log L_X \quad (1)$$

with a correlation coefficient  $\zeta = 0.980$ . As a comparison, we have also selected all the 47 GRBs, trying to

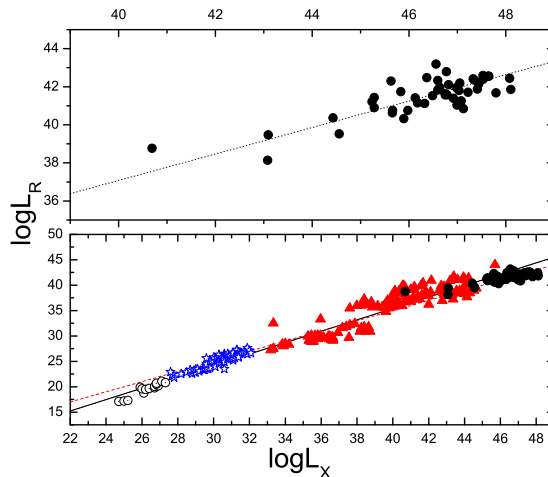


FIG. 1.— The upper panel includes only the GRBs and their best fitting linear correlation in black dotted line ( $L_R \simeq 1.94 \times 10^9 L_X^{0.695}$ ). The lower panel contains 15 solar flares (black dot circles), 65 cool stars (blue stars), 149 AGNs (red triangles) and 47 GRBs (black solid circles) objects in the  $L_R - L_X$  plane. The black solid line,  $L_R \simeq 3.42 \times 10^{-10} L_X^{1.122}$  is the best fit. The red dashed line indicates  $L_R = 10^{-5} L_X$ .

examine the correlation between  $L_R$  and  $L_X$ , the best fitting result is

$$\log L_R = (9.288 \pm 1.339) + (0.695 \pm 0.028) \log L_X \quad (2)$$

with a correlation coefficient  $\zeta = 0.814$ .

These correlations can be translated to

$$L_R \simeq 3.42 \times 10^{-10} L_X^{1.122}, \quad (3)$$

and

$$L_R \simeq 1.94 \times 10^9 L_X^{0.695}. \quad (4)$$

The correlation Eq.(1) coincide with Laor & Behar (2008), and also can be seen that the  $L_X/L_R = k \times 10^{15.5 \pm 0.5}$  correlation discovered by Benz & Güdel (1994) is confirmed in Eq.(4) with a slightly different slope. The slope of this correlation becomes flatter when the samples are expanded.

## 3. CONCLUSION AND DISCUSSION

The search of  $L_R$  and  $L_X$  in GRBs was done in this work. We found the  $L_R - L_X$  correlation for solar, cool stars and AGNs can be extended to GRBs. Even astrophysical phenomenons are divided into different classes, they still have common features on some properties. That implies they essentially may have some commonality. Franciosini & Chiuderi Drago (1995) presented a model of magnetic loop which only have one free parameter, the thermal plasma density, indicating a possible co-spatiality of the two emissions, radio emission and X-ray emission. On the other hand, the positive correlation between  $L_R$  and  $L_X$  is natural. However, the detailed underlying nature of this relation is still unclear.

Not like the other objects, the radio and X-ray data of GRBs are not simultaneous. The radio peak of GRB afterglows are generally at several days or even months, while the X-ray data are frozen to be at the 11 hours of the observer's frame. One reason is that the simultaneous data is very rare. Thanks to the fast corresponding of *Swift* XRT, the X-ray data can be obtained very quickly.

<sup>4</sup> [http://www.swift.ac.uk/xrt\\_products/index.php](http://www.swift.ac.uk/xrt_products/index.php)

But it also decays quickly, and fades out in a few days. There is no fast slewing radio telescope to observe the very early radio emission. Also notice the radio emission is always optically thick in the early stage, its luminosity is depressed and sensitively related to its size. Therefore, even occasionally the GRB location is inside the field of view of a radio telescope, it is very hard to be detected because of the faint luminosity. Later on, with the expansion of the GRB ejecta, the radio emission emerges while the X-ray fades away. That means the simultaneous radio and X-ray luminosities may not obey the proportional relation. From the light curves of GRB X-ray afterglows, the X-ray luminosity at 11 hours generally represents a typical X-ray emission. The correlation of the peak radio luminosity and X-ray luminosity at 11 hours may indicate their energy source origin should be

related, rather than microphysical radiation mechanisms. This extension to the various objects may also indicates the radio and X-ray emission may have the same engine while presenting in two different bands.

The fundamental plane between  $L_X$ ,  $L_R$  and  $M_{BH}$  is even tighter in stellar mass and supermassive black holes (Merloni et al. 2003). Though the GRB is believed harboring a stellar mass black hole, the fundamental plane is not extending to GRBs.

This work is supported by the National Natural Science Foundation of China (Grants No. U1231101 and 11173011), and the Guangxi Science Foundation (Grant No. 2014GXNSFBA118009).

## REFERENCES

- Amati, L., Frontera, F., Tavani, M. 2002, *A&A*, 390, 81  
 Anderson, G. E., van der Horst, A. J., Staley, T. D. et al. 2014 *MNRAS*, 440, 2059  
 Benz A., O., Güdel M. 1994, *A&A*, 285, 621  
 Benz A., O., Güdel M. & Schmitt, J. H. M. M. 1996, *ASPC*, 93, 291  
 Chandra, P. & Frail, D. A. 2012, *ApJ*, 746, 156  
 Cucchiara, A., Prochaska, J. X., Perley, D. et. al. 2013, *ApJ*, 777, 94  
 de Ugarte Postigo, A., Xu, D., Malesani, D., Gorosabel, J., Jakobsson, P., & Kajava, J. 2013, *GRB Coordinates Network*, 15187, 1  
 Flores, H. et al., 2013, *GCN Circ*, 14491  
 Fong, W., Berger, E., Metzger, B. D. et. al. 2014, *ApJ*, 780, 118  
 Francosini, E. & Chiuderi Drago, F. 1995, *A&A*, 297, 535  
 Ghirlanda Giancarlo, Ghisellini Gabriele, Lazzati Davide. 2004, *ApJ*, 616, 331  
 Ghirlanda, G., Nava, L., Ghisellini, G., et al. 2012, *MNRAS*, 420, 483  
 Güdel, M., Benz, A. O. 1993, *ApJ*, 405, 63  
 Güdel, M., Schmitt, J. H. M. M., Bookbinder, J. A. & Fleming, T. A. 1993b, *ApJ*, 415, 236  
 Güdel, M. 1996, *IAUS*, 176, 485  
 Klebesadel, R. W., Strong, I. B., Olson, R. A., Jun. 1973, *Observations of Gamma-Ray Bursts of Cosmic Origin*, *ApJ*, 182, L85.  
 Kruehler, T., Fynbo, J. P. U., Milvang-Jensen, B., Tanvir, N., & Jakobsson, P. 2012, *GCN*, 13134, 1  
 Kumar, Pawan, Zhang, Bing. 2014, arXiv1410.0679K  
 Laor, A., Behar, E. 2008, *MNRAS*, 390, 847  
 Lei, W.-H., Zhang B. & Liang E.-W., *ApJ*, 765, 125  
 Liang, E.-W., Yi, S.-X., Zhang, J., et al. 2010, *ApJ*, 725, 2209  
 Liang, Enwei & Zhang, Bing. 2005, *ApJ*, 633, 611  
 Linsky, J. L. 1996, *ASPC*, 93, 439  
 Lü Jing, Zou Yuan-Chuan, Lei Wei-Hua. et al. 2012, *ApJ*, 751, 49  
 Merloni, A., Heinz, S. & di Matteo, T. 2003, *MNRAS*, 345, 1057  
 Middleton, M. J., Miller-Jones, James C. A., Markoff, S., Fender, R., Henze, M. et al. 2013, *Nature*, 493, 187  
 Piran, T. 2004, *Rev. Mod. Phys.*, 76, 1143  
 Sanders, D. B., Phinney, E. S., Neugebauer, G., Soifer, B. T., Matthews, K. 1989, *ApJ*, 347, 29  
 Staley, T. D., Titterton, D. J., Fender, R. P. et. al. 2013, *MNRAS*, 428, 3114  
 van der Horst, A. J., Levan, A. J., Pooley, G. G. et al. 2015, *MNRAS*, 446, 4116  
 van den Oord, G. H. J. 1999, *ASPC*, 158, 189  
 Veres, Pter, Corsi, Alessandra, Frail, Dale A., Cenko, S. Bradley, & Perley, Daniel A. 2014, arXiv1411.7368  
 Wang, J.-Z., Lei, W.-H., Wang, D.-X., et al., 2014, *ApJ*, 788, 32  
 Wu, Q., Zou, Y.-C., Cao, X. et al., 2011, *ApJ*, 740, L21  
 Xu, D., et al. 2013, *GCN Circ*, 14478  
 Yonetoku, D., Murakami, T., Nakamura, T. 2004, *ApJ*, 609, 935  
 Zauderer, B. A., Berger, E., Margutti, R. et al. 2013, *ApJ*, 767, 161  
 Zhang, B., 2007, *ChJAA*, 7, 1

TABLE 1  
THE REDSHIFT, RADIO LUMINOSITY AND X-RAY LUMINOSITY OF THE GRBS.

GRB	$z$	$D_L^a$	$\nu_R^b$	$F_m^c$	$F_R^d$	$F_X^{11h\ e}$	$L_R^f$	$L_X^g$
970508	0.835	5299.32	8.46	958	8.10	5.7	27.23	1.92
970828	0.958	6288.80	8.46	144	1.22	19.9	5.76	9.42
980425	0.009	38.27	8.64	39360	340.07	2.8	0.060	0.000049
980703	0.966	6354.40	8.46	1370	11.59	14.0	56.0	6.76
981226	1.110	7558.88	8.46	137	1.16	2.8	7.92	1.91
990510	1.619	12108.32	8.46	255	2.16	34.7	37.84	60.87
991216	1.020	6800.95	15.00	1100	16.50	78.1	91.31	43.22
010222	1.477	10800.10	8.46	93	0.79	70.5	10.98	98.39
011211	2.140	17105.31	8.46	162	1.37	180.0	47.98	630.15
021004	2.330	18991.03	22.50	1614	36.32	8.4	1567.09	36.25
030226	1.986	15599.76	22.50	328	7.38	13.5	214.88	39.31
030329	0.169	804.57	43.00	59318	2550.67	548.6	197.56	4.25
031203	0.105	479.23	22.50	483	10.87	4.5	0.30	0.012
050401	2.898	24785.55	8.46	122	1.03	35.1	75.86	258.00
050416A	0.650	3887.37	8.46	373	3.16	25.3	5.71	4.57
050525A	0.606	3566.96	8.46	164	1.39	51.5	2.11	7.84
050603	2.821	23987.77	8.46	377	3.19	33.0	219.59	227.20
050730	3.968	36185.46	8.46	212	1.79	76.7	280.99	1201.64
050820A	2.615	21871.45	8.46	150	1.27	221.2	72.63	1266.05
050824	0.830	5259.90	8.46	152	1.29	13.7	4.26	4.54
050904	6.290	62311.66	8.46	76	0.64	0.5	298.70	23.23
051022	0.809	5095.05	8.46	268	2.27	426.5	7.04	132.47
060218	0.033	142.97	22.5	250	5.63	48.8	0.014	0.012
060418	1.490	10918.75	8.46	216	1.83	9.4	26.07	13.41
070125	1.548	11450.89	22.50	1778	40.01	37.8	627.63	59.30
071003	1.604	11968.90	8.46	616	5.21	55.7	89.32	95.47
071010B	0.947	6198.94	8.46	341	2.89	45.6	13.26	20.97
071020	2.146	17164.39	8.46	141	1.19	16.1	42.05	56.75
080603A	1.687	12743.86	8.46	207	1.75	15.8	34.03	30.70
090313	3.375	29800.55	8.46	435	3.68	31.9	391.04	338.96
090323	3.570	31883.30	8.46	243	2.06	28.1	250.04	341.78
090328	0.736	4531.37	8.46	686	5.80	61.4	14.26	15.08
090423	8.260	85417.81	8.46	50	0.42	5.0	369.27	436.49
090424	0.544	3126.69	8.46	236	2.00	2.3	2.34	0.27
090715B	3.000	25847.66	8.46	191	1.62	8.2	129.17	65.55
090902B	1.883	14605.36	8.46	84	0.71	47.0	18.14	119.96
091020	1.710	12960.08	8.46	399	3.38	19.5	67.84	39.19
100414A	1.368	9814.85	8.46	524	4.43	143.7	51.10	165.63
100418A	0.620	3668.21	8.46	1218	10.30	10.7	16.59	1.72
100814A	1.440	10463.72	7.90	613	4.84	82.0	63.44	107.42
100901A	1.408	10174.38	33.60	378	12.70	90.1	157.31	111.60
100906A	1.727	13120.28	8.46	215	1.82	27.1	37.46	55.82
111215A	2.060	16320.50	8.40	1340	11.26	140.0	358.73	446.30
120326A	1.798	13792.90	15.00	771	11.57	93.2	263.25	212.10
130427A	0.340	1783.10	15.70	4183	65.67	2167.6	24.98	82.46
130603B	0.3565	1882.80	6.70	118.6	0.79	8.5	0.34	0.36
130907A	1.238	8663.80	15.00	1060	15.90	308.1	142.80	276.74

NOTE. — a. Luminosity distance in unit of Mpc. b. The frequency of radio band in unit of GHz. c. The radio peak flux densities in unit of  $\mu\text{Jy}$ . d. The radio peak flux in unit of  $10^{-20} \text{ erg cm}^{-2} \text{ s}^{-1}$ . e. X-ray flux at 11hr in unit of  $10^{-13} \text{ erg cm}^{-2} \text{ s}^{-1}$ . The fluxes are measured in 0.3-10 keV energy range. f. The radio luminosity of radio band, in unit of  $10^{40} \text{ erg s}^{-1}$ . g. The 11hr X-ray luminosity, in unit of  $10^{45} \text{ erg s}^{-1}$ .